Remote Sensing Products for Ocean Applications

William Y. Tseng*, Robert N. Stone*, William G. Pichel*, Ralph Meiggs*,
Pablo Clemente-Colón*, Antony K. Liu** and Sunny Wu**

*NOAA/NESDIS Washington, D.C. 20233, USA
Tel.: (301) 763-8142; Fax: (301) 899-9196
E-Mail: william.tseng@noaa.gov

**NASA/GSFC, Code 971, Greenbelt, MD 20771, USA
Tel.: (301) 614-5714; Fax: (301) 614-5644
E-Mail: liu@neptune.gsfc.nasa.gov

Abstract

Considering the usefulness of remote sensing products to coastal ocean research and applications, the National Oceanic and Atmospheric Administration, National Environmental Satellite, Data, and Information Service (NOAA/NESDIS) has devoted considerable resources to develop several remote sensing products, including the Sea Surface Temperature (SST) from the NOAA Advanced Very High Resolution Radiometer (AVHRR) for the NOAA CoastWatch Program, and, more recently, experimental SST from the Geostationary Operational Environmental Satellite (GOES), ocean turbidity and chlorophyll-a from the Sea-viewing Wide Field-of-view Sensor (SeaWiFS), and wind speeds, wind vectors and ship detection from RADARSAT Synthetic Aperture Radar (SAR) data. This paper illustrates briefly those products and their usefulness, and presents examples of the application of some of those products for the tracking and monitoring of ocean surface mesoscale features which include current boundaries, eddies or rings, and red tides, as well as ocean wind speed, wind vector, and ship detection products. The areas of illustration are focused in the coastal oceans in the northeast and southeast of the United States, the coast of Alaska, and the Gulf of Mexico.

1. Introduction

The NOAA CoastWatch program was established in1987 to deal with a strong red tide occurring along the eastern coast of North America. In conjunction with NOAA Line and Program Offices, NOAA's CoastWatch program has operationally provided near real-time environmental satellite data and products to federal, state, and local coastal resource managers, marine scientists, educators and public users. Products are supplied in direct support of NOAA and other agency mission requirements in the coastal areas of the eight USA CoastWatch Regional Nodes as shown in the Figure 1. CoastWatch satellite data provide users with valuable information needed to quickly respond to environmental events and minimize the resulting economic and environmental impacts. More recently, the NOAA/NESDIS Ocean Remote Sensing program was established in order a capability to utilize the many new remote sensing data streams to generate several kinds of ocean remote sensing products: 1) Experimental SSTs from GOES satellites for the eight US CoastWatch Regional Nodes, 2) Surface wind speed, wind vector and ship detection products from RADARSAT SAR data off the coast of Alaska for the pre-operational Alaska SAR Demonstration, and 3) Turbidity and chlorophyll-a products from SeaWiFS data in the coastal areas of CoastWatch Nodes. All these products are now available for qualified users to coastal ocean research and operational applications with access provided over the Internet. The paper will be limited to these three products. Many other ocean remote sensing products are also available from NOAA. Refer to the following website for detailed NOAA/NESDIS consolidated product list:
http://osdacces.nesdis.noaa.gov:8081/ppit/cpl/cpl.cfm

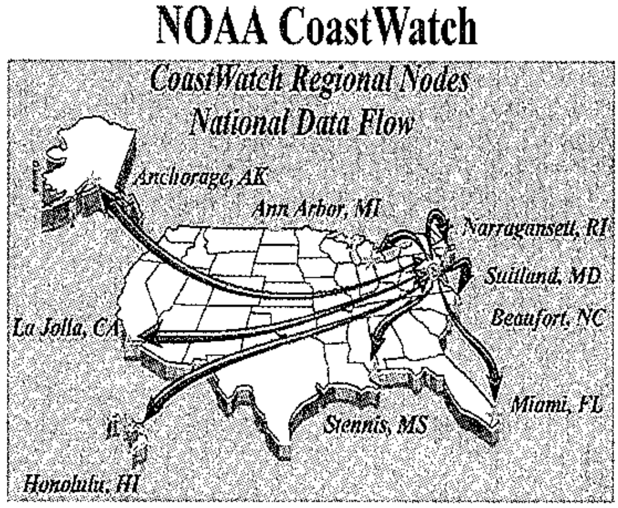

Figure 1. NOAA CoastWatch Regional Nodes

2. Ocean Remote Sensing Products

2.1. Sea Surface Temperature Products from NOAA and GOES

NOAA's remote sensing SST products are derived from NOAA AVHRR or GOES data. Two general multichannel algorithms have been derived and used operationally, the NOAA multichannel SST (MCSST) and nonlinear SST (NLSST). MCSST demonstrated a consistent global root mean square difference accuracy less than 0.7 °C (Strong and McClain, 1984; McClain, 1989). Operational retrieval algorithms are empirically derived by regressing satellite channel brightness temperature retrievals with global drifting buoy SST measurements within specified time and distance constraints. The NLSST was introduced (Walton et al., 1990 and 1998). Since the coefficient of the second term of MCSST equations, called the gamma parameter, is not a constant but actually a function of both scene temperature and water vapor amounts (Walton, 1988). Recent validation for US coastal waters (Pichel, et al., 1995), for NOAA-14, showed the mean difference between satellite-buoy SST matches was 0.31 °C during the day and 0.27 °C at night with a standard deviation of 0.57 °C during the day and 0.59 °C at night. For NOAA-15 global operational NLSST, the bias was 0.14 °C and 0.08 °C for the day and night algorithms, respectively. The standard deviation was 0.5 °C or less (Li, et al., 2000). The general forms of NLSST and MCSST algorithms for NOAA satellites for CoastWatch Regional Nodes are as follows:

$$NLSST = AT_4 + B(T_4-T_5)(MCSST) + C(T_4-T_5)(Sec\theta - 1) + D$$
$$MCSST = ET_4 + F(T_4-T_5) + G(T_4-T_5)(Sec\theta - 1) + H$$

Where A, B, C, D, E, F, G, and H are coefficients to be determined by regression equations of satellite and buoy data matches; T_4, and T_5 are the Channel 4 (11 μm) and Channel 5 (12 μm) temperatures, respectively, in Kevin, and Secθ is the secant of the satellite zenith angle. The coefficients for NOAA-12, -14, and -15 for the CoastWatch Nodes are listed in Table 1 in the Appendix. Further information and the validation of the data can be found at the following website: http://manati.wwb.noaa.gov/sst/cwIntroduction.html.

The United States normally operates two meteorological satellites in geostationary orbits over the equator. Each satellite views almost a third of the Earth's surface: the one monitors the North and South America and most of the Atlantic Ocean, the other the North America and the Pacific Ocean basin. GOES-8 (or GOES-East) is positioned at 75°W longitude and at the equator while GOES-10 (or GOES-West) is positioned at 135°W longitude and at the equator. The two operate together to produce a full-face picture of the Earth, day and night. Coverage extends approximately from 20°W longitude to 165°E longitude. There are five channels of GOES Imager, centered in wavelength ranges at 0.7 μm for Channel 1, 3.9 μm for Channel 2, 6.7 μm for Channel 3, 10.7 μm for Channel 4, and 12.0 μm for Channel 5. The wavelength ranges of the channels are quite similar to those of the NOAA-AVHRR. The experimental Algorithms for GOES SST for GOES-8 and -10 satellites are, respectively:

$$SST= -6.4110 + 1.0260T_4 + 1.1900 (T_4 -T_5) + 0.2017 (T_4 - T_5)^2$$
$$SST=18.3500 + 0.9459T_4 + 0.4261(T_4 - T_5) + 0.4473 (T_4 - T_5)^2$$

Where T_4 and T_5 are Channel 4 (10.7 μm) and Channel 5 (12.0 μm) temperatures, respectively, for GOES satellites. These regression equations were verified by comparing GOES and buoy SST. The mean bias (GOES SST-Buoy SST) for GOES-8 is -0.05°C with a standard deviation of 0.79°C. The GOES-10 mean bias is 1.041 with a standard deviation of 0.94°C (Maturi, Li, and Wu, 2000). Further validation of the experimental GOES-SSTs will be continued. Refer to the website for more information: http://orbit35i.nesdis.noaa.gov/orad/eil/sst_algorithm.html.

SST is one of the most important ocean physical properties. Important applications are, but not limited to, coastal ocean circulation, upwelling, tracking of current features, fishery mapping, input data for ocean modeling, detection of river plumes, tracking of iceberg and sea ice, coral reef bleaching studies and detection of ocean hazards or oil spills.

2.2. RADARSAT SAR Products

In order to provide near real-time SAR data, NOAA in partnership with the National Ice Center (NIC) has augmented_existing satellite reception and processing facilities at the Alaska SAR Facility (ASF). Access is available to SAR data from the Canadian RADARSAT-1 satellite carrying a C-band (5.6-cm), acquired by ASF in Fairbanks, Alaska, by the Canadian readout stations in Gatineau, Quebec and Prince Albert, Saskatchewan, the Norwegian station in Tromso, and the West Freugh station in Scotland. The data are transferred from the ASF via a dedicated T1 link to the Satellite Active Archive (SAA) in Suitland, MD. Using those data, several RADARSAT SAR products are generated initially as near real-time pre-operational products for the Alaska SAR Demonstration, including: SAR imagery, ocean surface wind measurement from SAR, and ocean vessel position detection Ancillary products are also provided to adequate interpretation of SAR imagery and derived products, including other available satellite, surface, and model environmental data (Pichel and Clemente-Colón, 2000).

SAR imagery products are made available to users via a web server and through an Internet-based image processing, analysis, and archiving system, known as the WWW image Processing Environment (WIPE) developed by Applied Coherent Technology Corporation. The WIPE system ingests near-real-time SAR imagery and catalogues the data in a database for subsequent queries by the end-user running an Internet browser on a PC or UNIX computer. The system allows the user to download or browse SAR-derived products, and ancillary data, do image processing and analysis, create data cubes of collocated image, vector, and point data, and output or download data cubes or selected individual data sets.

The algorithm for SAR wind imagery products used in the Alaska Remote Sensing SAR Demonstration is based on a modified CMOD4 wind model developed by the Johns Hopkins University Applied Physics Laboratory (JHU/APL) (Thompson and Beal, 2000; Monaldo, 2000). The CMOD4 model was modified for the horizontal transmit, and horizontal receive (HH) polarization of the RADARSAT SAR. Accurate wind estimates from this algorithm require the knowledge of the wind direction, the angle between the wind direction and the radar look direction, and the SAR incidence angle, as well as accurate normalized radar coss section measurements. In the pre-operational wind procedure being developed, wind direction is obtained from a model wind analysis or forecast, currently from the Navy Fleet Numerical Meteorology and Oceanography Center (FNMOC). A second wind product for the demonstration, known as the SAR wind vector, was developed by Veridian ERIM International, using another approach. Fast Fourier transforms (FFT) are performed on sections of the image to generate surface wind spectra. The direction of the wind is determined from the peak in the spectra or the smear of energy in the crosswind direction. The wind speed is determined with an algorithm similar to that used for the SAR wind images. Refer to the following on-line website for more information: http://orbit35i.nesdis.noaa.gov/orad/sar/

Ships are generally visible from SAR imagery, because they appear as bright targets with a contrast that depends on the background ocean backscatter. The contrast varies with ocean conditions such as surface wind speed, waveheight, and the presence of ocean features and with the SAR viewing geometry. Because of the varying contrast, a Constant False Alarm Rate (CFAR) algorithm is used in which to a detection threshold varies over the image and depends on the local background backscatter statistics. Some false detections are due to small islands not in the land data base or broken ice pieces along the ice edge.

In addition to ocean surface winds and ship detection, SAR imagery has many other applications, such as, tracking of ocean features, detection of natural and man-made ocean pollution, measurement of surface and internal waves, tracking of iceberg and sea ice, and mapping of algal blooms. Many other applications in hydrology, geology, geography and meteorology have also been noted.

2.3. Ocean Color Products

NOAA CoastWatch obtains SeaWiFS data from either the NASA/GSFC SeaWiFS project for authorized research purposes or OrbImage via purchase under the NOAA-OrbImage Contract. Ocean color data products are processed from SeaWiFS Level 1A data to unmapped but georeferenced Level 2 products for the eight CoastWatch Regional Nodes. CoastWatch ocean color products include SeaWiFS images of seven channels, which are centered at 412, 443, 490, 510, 555, 670 and 865 nm, ocean turbidity and chlorophyll-a concentration.

The experimental algorithm for the turbidity product used in CoastWatch ocean color uses the reflectance for band 5 (555 nm), which provides a good measure of turbidity over a range of water clarity and provides a measure of sediment loads in the water. This algorithm was recommended by Rick Stumpf as indicated in the following website. The experimental algorithms for chlorophyll-a products for CoastWatch use three kinds of algorithms developed by several developers (O'Reilly, et al., 1998; Stumpf, et al., 2000) applied to different U.S. coastal regions. Color products for the northeast and west of U.S., the Great Lakes, and Hawaii are generated by NASA's algorithm, those for the southeast US and the Gulf of Mexico by Stumpf's algorithm, and those for the Alaska by Eslinger's algorithm. The CoastWatch chlorophyll-a algorithms are constantly being updated, based on changes recommended by the above developers. Their changes are not just in the calculation, but also what and how corrections may be applied. Refer to the references indicated and the following website for more information: http://wwwo2c.nesdis.noaa.gov/ocolor/owelcom.htm

Ocean color data have been used by the oceanographic community for the study of ocean primary production and global biogeochemistry. Primary production refers to the organic material in the sea that is produced by primary producers which include algae and some bacteria, and exist at the lowest level of the food chain. The concentration of the microscopic marine plants, called phytoplankton, can be derived from satellite observation of ocean color. This is due to the fact that the color in the word's oceans in the visible light region (wavelengths of 400-700 nm) varies with the concentration of chlorophyll and other plant pigments present in the water. The more phytoplankton presents in the water, the greater the concentration of the plant pigments and the greener the water will be. Turbidity and chlorophyll-a of the sea water reflect that the water clarity index which is determined by the absorption due to live phytoplankton, dissolved pigments, and detrital pigments, and the scattering due to suspension particles.

3. Examples

Several examples were selected to illustrate the usefulness and applications of the products indicated in Section 2.

3.1 SST from AVHRR and GOES

One of the clearest AVHRR SST images from NOAA-12, on June 11, 1977 is shown in Figure 2 revealing different water masses in the Gulf Stream, meandering boundaries, and eddies at the boundary. This quantitative and qualitative information is useful for current dynamical studies, circulation, and many other physical oceanography and fishery applications. As a GOES SST composite of three hourly images in the Gulf of Mexico, Figure 3 clearly shows the water masses of different SSTs and the position of the Loop Current. GOES is sensing the Earth almost continuously, so GOES images are able to track ocean different features in near real time.

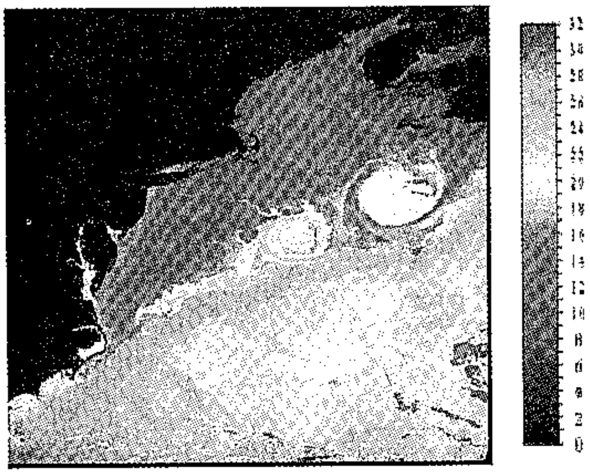

Figure 2. CoastWatch AVHRR SST at the resolution of 4.17 km in the Gulf Stream area (Latitude from 29.94 to 45.82 °N and Longitude from 56.81 to 79.08 °W). SSTs are in degrees Centigrade. boundary. The highest SSTs in the Gulf Stream shown in the image are a bout 30°C.

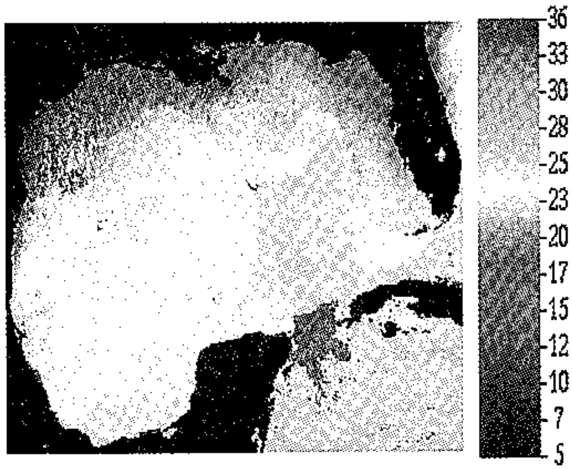

Figure 3. CoastWatch experimental GOES SST, at the resolution of 6 km at the Equator for the Gulf of Mexico area (Latitude from 17.82-31.02°N and Longitude from 79.73-98.23°W). SSTs are in degrees Centigrade.

3.2. RADARSAT SAR Wind and Ship Detection Products

The following SAR wind speed imagery in Figure 4 was generated by JHU/APL using the CMOD4 model off the Coast of Russia. The large arrows represent the model wind speed. The arrow color is related to the wind speed and orientation. The small arrows are the wind speed (color) and direction determined by the Veridian ERIM International SAR wind algorithm.

The next two figures are a wind vector image (Figure 5) and a ship detection image (Figure 6) generated by the Veridian ERIM International, Inc. off the coast of the Alaska Peninsula, using SAR wind vector and ship detection algorithms.

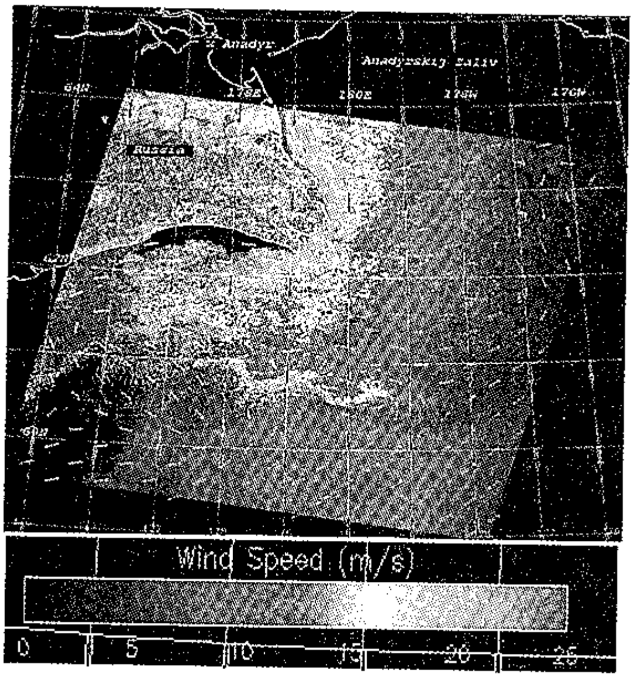

Figure 4. SAR wind speed image showing maximum winds up to 25 m/s off the coast of Russia (61.5N and 179.3E) in April 13, 2000, at 18:29:43 GMT.

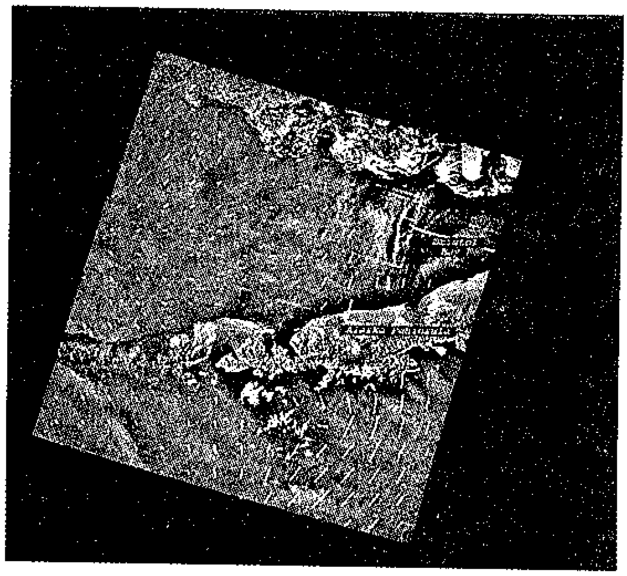

Figure 5. Wind vector imagery generated by Veridian ERIM International, off the coast of the Alaska Peninsula on March 31, 2000, at 04:25:14 GMT.

3.3. Turbidity and Chlorophyll-a Concentration from SeaWiFS

At the end of September and the beginning of October 1999, Florida's east and west coasts were hit by a widespread outbreak of potentially toxic red tide blooms. Local officials reported that there were algal blooms off Florida's west coast near Sarasota, and on the west coast near the city of Jacksonville. Part of the red tide also reached coastal areas of North Carolina and Texas. In Figures 7 and 8, red tides are clearly shown by the high turbidity and chlorophyll-a concentration off the coastal areas of Florida.

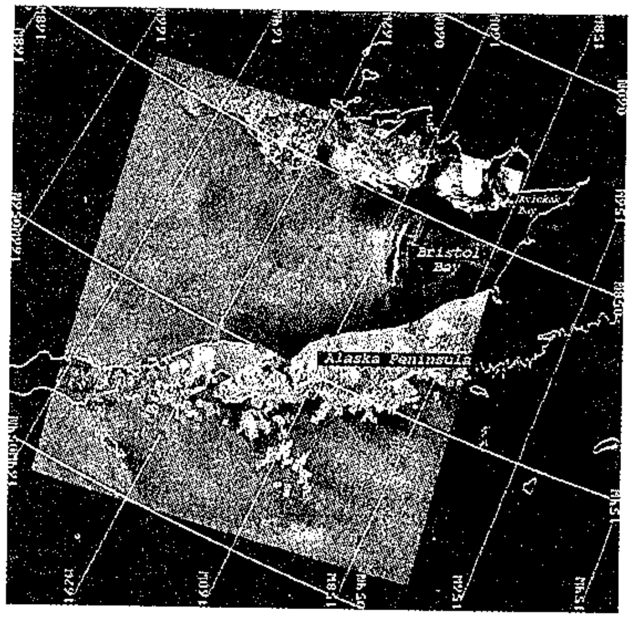

Figure 6. Ship detection imagery generated by Veridian ERIM on March 31, 2000. (In the original color image, a triangle means a ship was detected outside of a 2km land border, while a square means the detection was within the 2km border near the land. A green symbol means the detection was statistically larger enough so that it is fairly certain it is a ship, while a red symbol indicates a weaker target.)

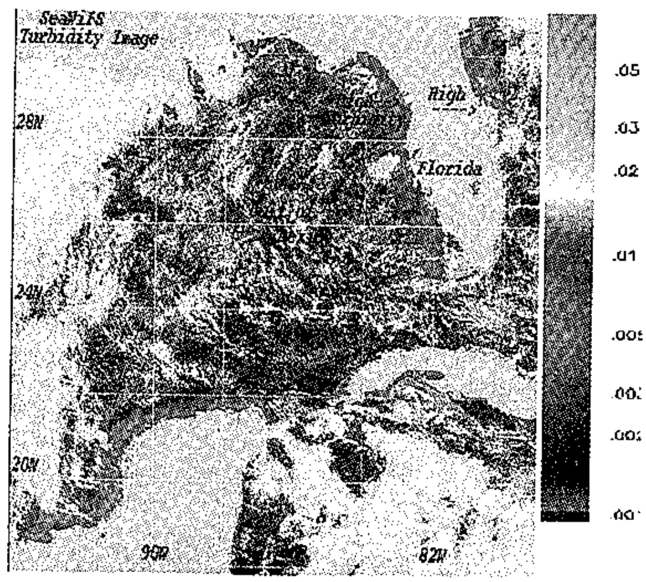

Figure 7. CoastWatch SeaWiFS turbidity product, in Inverse Steradian (sr^{-1}), on September 28, 1999, in the Gulf of Mexico, showing higher turbidity in the areas of red tides.

4. Summary

This paper introduced NOAA remote sensing products for ocean applications, specially focused on those in the U.S. coastal ocean regions. Three important products were selected: SST products from AVHRR and GOES, wind speed, wind vector and ship detection products from RADARSAT SAR, and turbidity and chlorophyll-a products from SeaWiFS. Some imagery products were presented to illustrate their usefulness. NOAA scientists are continuing to develop these and other ocean products. Many other remote sensing ocean products, both in coastal regions and the open ocean, are also available from NOAA for ocean research and applications.

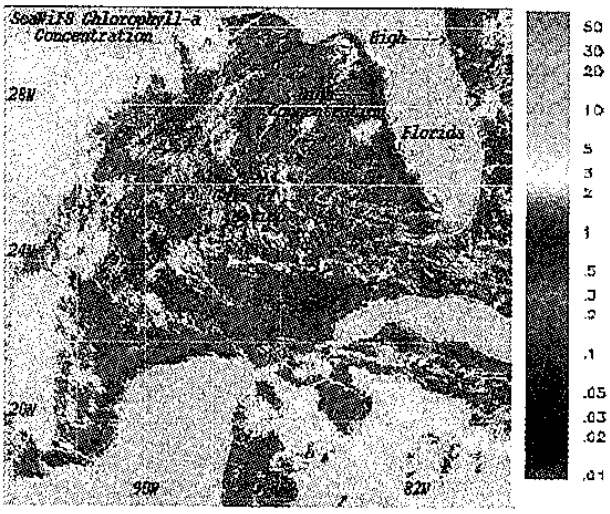

Figure 8. SeaWiFS generated chlorophyll-a concentration, in mg/m^3, on September 28, 1999, showing high chlorophyll-a in eastern and western coasts of Florida.

5. Acknowledgment

The authors would like to thank Rick Stumpf for providing his unpublished paper for our reference, and for explaining the difference in turbidity units between AVHRR and SeaWiFS products, to Xiaofeng Li for providing his unpublished paper on the global operational NLSST algorithm for NOAA-15, and to Michael Soracco for his explanation of units in the products of turbidity and chlorophyll-a. In addition, the authors would like to express their appreciations to Michael Matson for his valuable comments on the paper. Financial support from NOAA/NESDIS Ocean Remote Sensing Program is highly appreciated.

6. Reference

Li, X., W. Pichel, E. Maturi, P. Clemente-Colón, and J. F. Sapper, "Deriving the Operational Nonlinear Multi-channel Sea Surface Temperature Algorithm Coefficients for NOAA-15 AVHRR/3," Submitted to the *International J. Remote Sensing, Remote Sensing Letters*, January 2000.

Maturi, E., X. Li, and X. Wu, "GOES Sea Surface Temperature Products in NOAA/NESDIS," *10th Conference on Satellite Meteorology and Oceanography*, Long Beach, CA, p. 141-143, 9-14 January 2000.

May, D. A. Global and Regional Comparative Performance of Linear and Nonlinear Satellite Multichannel Sea Surface Temperature Algorithms, *Naval Research Laboratory*, NRL/MR/7240-93-7049, September 1993.

McClain, E. P., "Global Sea Surface Temperatures and Cloud Clearing for Aerosol Optical Depth Estimates," *Int. J. Remote Sens*. 10:763-769, 1989.

Monaldo, F., "The Alaska SAR Demonstration and Near-Real-Time Synthetic Aperture Radar Winds," *Johns Hopkins APL Technical Digest*, Vol. 21 No. 1, p.75-79, January-March 2000.

O'Reilly, J. E., S. Maritorena, B. G. Mitchell, D. A. Siegel, K. L. Carder, S. A. Garver, M. Kahru, and C. McClain, "Ocean Color Chlorophyll Algorithms for SeaWiFS," *J. Geophys. Res.*, Vol. 103, No. C11, p. 24,937-24953, October 1998.

Pichel, W. G., and P. Clemente-Colón, "NOAA SAR Applications and Demonstration," *Johns Hopkins APL Technical Digest*, Vol. 21 No. 1, p.49-57, January-March 2000.

Pichel, W. G., P. Clemente-Colón, J. F. Sapper, C. Duda, and V. M. Krasnopolsky, "Validation and Quality Control of CoastWatch Satellite-Derived Water-Surface-Temperature Imagery," Presented at *the Third Thematic Conference on Remote Sensing for Marine and Coast Environments*, Seattle, Washington, September 1995.

Strong, A., and E. P. McClain, 1984, "Improved Ocean Surface Temperatures from Space-Comparisons with Drifting Buoys," *Bull. Amer. Meteor*. 27:115-124, 1984.

Stumpf, R., et al., "SeaWiFS Ocean Color Data for US Southeast Coastal Waters," Preprint, *Proceedings, 6th International Conference Remote Sensing for Marine and Coastal Environments*, Charleston, SC., May 1-3, 2000.

Thompson, D. R, and R. C. Beal, "Mapping High-Resolution Wind Fields Using Synthetic Aperture Radar," *Johns Hopkins APL Technical Digest*, Vol. 21 No. 1, p.58-67, January-March 2000.

Walton, C. C., "Nonlinear Multichannel Algorithms for Estimating Sea Surface Temperature with AVHRR Satellite Data," *J. Appl. Meteor*. 27:115-124, 1988.

Walton, C. C., E. P. McClain, and J. F. Sapper, "Recent Changes in Satellite-Based Multi-Channel Sea Surface Temperature Algorithms," *Marine Technology Soc. Meeting Proceedings*, Washington, D. C., 1990.

Walton, C. C., W. G. Pichel, J. F. Sapper and D. A. May, "The Development of Operational Applications of Nonlinear Algorithm for the Measurement of Sea Surface Temperatures with the NOAA Polar-Orbit Environmental Satellite," *J. Geophys. Res.*, Vol. 103, No. C2, p. 27999-28012, 1998.

Appendix

Table 1. Coefficients for NOAA CoastWatch SST Algorithms

Satellite	Daytime/ Nighttime	A	B	C	D
NOAA-12	Day	0.876992	0.083132	0.349877	-236.667
	Night	0.888706	0.081646	0.576136	-240.229
NOAA-14	Day	0.939813	0.076066	0.801458	-255.165
	Night	0.933109	0.078095	0.738128	-253.428
NOAA-15	Day	0.913116	0.0905762	0.476940	-246.877
	Night	0.922560	0.0936114	0.548055	-249.819
		E	**F**	**G**	**H**
NOAA-12	Day	0.963563	2.579211	0.242598	-263.006
	Night	0.967077	2.384376	0.480788	-263.94
NOAA-14	Day	1.017342	2.139588	0.779706	-278.43
	Night	1.029088	2.075385	0.752567	-282.24
NOAA-15	Day	0.964243	2.71296	0.387491	-264.443
	Night	0.976789	2.77072	0.435832	-266.290